Research Square

Preprints are preliminary reports that have not undergone peer review.
They should not be considered conclusive, used to inform clinical practice,
or referenced by the media as validated information.

Experimental Investigation of Sodium Citrate Assisted Electrolyte in Electrochemical Machining of AISI 304 Stainless Steel

Nethaji Subash Chandra Bose Ayyavoo
Sona College of Technology
Saravanan Kandasamy Ganesan
Sona College of Technology
Vinod Kumaar. J. R
jrvinod@gmail.com
Dr.N.G.P. Institute of Technology
Karthick. S
Excel Engineering College
Jegadheesan. C
Kongu Engineering College
Venugopal. P
Muthayammal Engineering College Rasipuram

Research Article

Keywords: Sodium nitrate, Machining rate, Overcut, Palladium-coated electrode, Dimensional accuracy

Posted Date: November 17th, 2026

DOI: https://doi.org/10.21203/rs.3.rs-11275386/v1

License: This work is licensed under a Creative Commons Attribution 4.0 International License.
Read Full License

Additional Declarations: No competing interests reported.

Experimental Investigation of Sodium Citrate Assisted Electrolyte in Electrochemical Machining of AISI 304 Stainless Steel

Nethaji Subash Chandra Bose Ayyavoo[1], Saravanan Kandasamy Ganesan[2], Vinod Kumaar. J. R[3*], Karthick.S[4], Jegadheesan.C[5], Venugopal. P[6]

[1,2]*Department of Mechatronics Engineering, Sona College of Technology, Salem-636007, India,*

[3]*Department of Mechanical Engineering, Dr.N.G.P. Institute of Technology, Coimbatore, 641048, India, email: jrvinod@gmail.com*

[4]*Department of Mechanical Engineering, Excel Engineering College, Komarapalayam - 637 303, India, email: karthicksekar07@gmail.com*

[5]*Department of Mechatronics Engineering, Kongu Engineering College, Perundurai, Erode - 638060, India, email: cjegadheesan.auto@kongu.ac.in*

Department of Mechanical Engineering, Muthayammal Engineering College Rasipuram, Namakkal-637408, India,email:venunaveen73@gmail.com

[*]Corresponding author: *jrvinod@gmail.com*

Abstract

This study experimentally explores the influence of adding sodium citrate (Na_3Cit) to a sodium nitrate ($NaNO_3$) electrolyte in electrochemical machining (ECM) of AISI 304 stainless steel when using a palladium-coated tool electrode. The machining voltage, duty cycle, and electrolyte concentration were adjusted, while the machining rate (MR) and overcut (OC) were assessed. Raising the voltage from 6 to 11 V increased the MR from 0.20 to 0.42 μm/ s for $NaNO_3$; however, $NaNO_3$ + Na_3Cit reached 0.52 μm/ s at 11 V, which is about 24% higher. Within the same range, OC dropped from 343 to 221 μm for $NaNO_3$ and from 302 to 204 μm for the mixed electrolyte. At a 90% duty cycle, the $NaNO_3$ + Na_3Cit mixture achieved an MR of 0.35 μm/s, compared to 0.30 μm/s for $NaNO_3$ alone; meanwhile, OC dropped to 220 and 240 μm, respectively. At an electrolyte concentration of 0.41 mol/L, the MR was 0.46 μm/ s for the mixed electrolyte and 0.44 μm/ s for $NaNO_3$, with corresponding OC values of 210 and 230 μm. SEM observations showed cleaner, nearly circular holes with less sludge and sharper edge definition when using $NaNO_3$ + Na_3Cit. The results show that citrate-enhanced electrolyte boosts MR, dimensional accuracy, and electrochemical stability by enhancing complexation, optimizing current distribution, facilitating removal of reaction products, and better localizing anodic dissolution.

Keywords: Sodium nitrate; Machining rate; Overcut; Palladium-coated electrode; Dimensional accuracy

INTRODUCTION

In Electrochemical machining (ECM) electrolyte serves as the conductive medium that permits anodic dissolution of the workpiece. ECM finds application in various fields such as biomedical, aerospace and finishing of industrial components. The machining rate (MR), machining precision, surface finish, tool life, and overall process stability are all directly impacted by the electrolyte's selection and characteristics. To understand the behaviour of the electrolytes, many researchers have used different types of electrolytes. The electrochemical

dissolving behaviour of nitinol in various electrolytes for micro-ECM was examined by Sethi et al. (2022). The first three electrolytes, sodium chloride (NaCl), sodium nitrate ($NaNO_3$), and sodium bromide (NaBr), were all aqueous neutral electrolytes. A microchannel with the lowest average surface roughness of 0.848 µm was successfully created using aqueous $NaNO_3$ out of the three aqueous electrolytes. Micro-holes have been drilled over the MONEL 400 alloy work material by Gokulanathan and Annamalai (2024). Multi-objective optimization based on ratio analysis (MOORA) and VlseKriterijumska Optimizacija I Kompromisno Resenje are used to optimize the findings. The experiment combination of 50% duty cycle, 11 V machining voltage, and 28 g/l electrolyte concentration is the best optimal parameter solution. The electrolyte contributes 62.6% to machining performance, according to the ANOVA table of both. Zishanur Rahman et al. (2022) employed a variety of electrolyte materials, including sodium hydroxide (NaOH), Nitric acid (HNO_3), NaBr, Potassium hydroxide (KOH), sulphuric acid (H_2SO_4), NaCl, $NaNO_3$, and hydrochloric acid (HCl). They discovered that KOH(Aq.) and NaOH (Aq.) electrolytes are appropriate to produce tungsten microtools using the µECM process. Sriram et al. (2025) examined the optimization of micro-hole production in scrapped wheel alloy. The effects of electrolyte type on machining performance were assessed using potassium chloride, $NaNO_3$, and sodium chloride. Using the Taguchi-Grey relation analysis approach, voltage, duty cycle, and electrolyte concentration were optimized to maximize material removal rate (MRR) and reduce overcut (OC). With a MRR of 2.752 g/min and an OC of 0.068 mm, the ideal process parameters were identified as 14 V, DU of 85%. He et al. (2023) suggested using polyacrylamide (PAM), a non-Newtonian fluid, as the electrolyte. A high-quality micro-hole array with an average diameter of 330.11 µm, an average depth of 16.13 µm, and a depth-to-diameter ratio of 0.048 was produced. Experiments revealed that the mixed electrolyte (PAM–NaOH) had both the physical properties of a non-Newtonian fluid and the benefits of a conventional electrolyte to dissolve processing products, and it successfully increased the processing accuracy of masked ECM for 304 stainless steel (SS). Several organic electrolytes, including tartaric acid ($C_4H_6O_6$), citric acid ($C_6H_8O_7$), and a mixture of tartaric and citric acid (mixed electrolyte), have been employed in ECM by Kumaar et al. (2022). MRR and OC are used to assess ECM's performance. For the parameter combination of 12 g/l, 11 V, and 85%, the OC of tartaric acid electrolyte is 179% lower than that of mixed electrolyte. However, with parameter solutions of 25%, 11 V, and 20 g/l, the mixed electrolyte exhibits 114.2% more MRR than the tartaric acid electrolyte. In the ECM of SS316, Vian Nihad Najm et al. (2025) employed an environmentally friendly acidic sodium nitrate solution electrolyte. According to the findings, the voltage had the strongest influence on MRR and surface roughness (SR), followed by acidified sodium nitrate concentration. It was found that a voltage of 30 V, an electrolyte concentration of 100, and a gap of 0.2 mm produced a greater MRR (0.0823). Furthermore, a voltage of 30 V, an electrolyte concentration of 125, and a gap of 0.3 mm produced the lowest surface roughness (0.1881 µm).Gunasekaran et al. (2026) made a solution of 30% ethylene glycol and 70% distilled water with $NaNO_3$ and stainless-steel electrodes covered with polyvinyl acetate and ceramic paste that is sold commercially. The stainless-steel electrode at 9 V, 70% duty cycle, and 28 $g.L^{-1}$ electrolyte concentration and the ceramic coated electrode at 13 V, 80% duty cycle, and 28 $g.L^{-1}$ electrolyte concentration are the ideal parameter combinations for both electrolytes, according to the multi-criteria decision-making technique. In ECM, Gunasekaran et al. (2023) conducted tests

based on the Taguchi approach. The MRR and OC were calculated using the workpiece weight and hole diameter measurements, and experiments were conducted by altering the control parameters such as electrolyte concentration, voltage, and duty cycle. While the electrolyte concentration and voltage both demonstrate an even-increasing contribution to material removal, the voltage exhibits an intensifying tendency. While the cross over with voltage exhibits a better contribution to the MRR, the duty cycle has less of an effect. The duty cycle follows the worsening trend for the overcut in the electrolyte concentration. 20 V, 40 g/L, and 41% duty cycle are the ideal conditions to attain maximum MR and minimum OC. In this study, Janardhanan and Perianna (2024) used a dual fluid system as a unique machining technique to manufacture SS304. Aqueous solutions of NaCl, $NaNO_3$, $NaHCO_3$, $C_{12}H_{22}O_{11}$, and distilled water were utilized in the secondary fluid system. The taper angle, radial OC, MRR, surface roughness, and radial-stray current impacted zone were used to assess the output responses. It has several benefits, such as enhanced surface finish, better control over the machining process, and a lower risk of pit formation at the hole's entry side. Sankar et al. (2017) examined the effects of NaCl electrolyte at different concentrations (10–30%) in conjunction with silicon carbide abrasive particles on the MR, SR, and radial OC. Because the rate of dissolution was greater, this study definitively concluded that electrolyte concentrations up to 20% showed a favourable impact in the MRR for the machining of composites. Ayyappan and Sivakumar (2014) investigated how an oxygenated aqueous NaCl electrolyte could improve the ECM process's performance. With machining conditions of voltage of 17 V, tool feed rate of 0.5 mm/min, and electrolyte concentration of 142.5 g/l of water, the oxygenated NaCl environment yields the largest MR of 7.33 g/min with SR an of 1.90 μm, while the aqueous NaCl environment yields MR of 1.98 g/min and SR an of 3.13 μm. In this research two types of electrolytes were used namely $NaNO_3$, and sodium citrate ($Na_3C_6H_5O_7$). The effect of these electrolytes on the MR, and OC were analysed.

EXPERIMENTAL SETUP

Machining voltage, duty cycle, and electrolyte concentration among other process parameters that influence ECM performance are regarded as input factors. These parameters were selected according to their impact on surface integrity, dimensional accuracy, MR, machining stability, and the electrochemical dissolution process. Preliminary experiments and existing literature were reviewed to identify a stable machining window that avoids undesirable effects such as arcing, overheating, passivation, and stray-current machining. A stitching needle, serving as a 500 μm diameter tool electrode, was employed, along with a 0.5 mm thick 304 SS workpiece, in the study. The selection of machine parameters significantly affects the ECM process's accuracy, stability, and efficiency. The machining voltage (6-11 V), duty cycle (40-90%), and electrolyte concentration (0.12 - 0.41 M $NaNO_3$ sodium citrate solution) employed in this study were selected according to existing literature and electrochemical principles [Dong et al. 2026, Qin et al. 2024]. The selected ranges were intended to reduce passivation, stray-current machining, excessive gas production, and thermal effects, while ensuring stable electrochemical dissolution. Palladium is applied to the needle through sputtering. Figure 1 displays the palladium coated tool electrode.

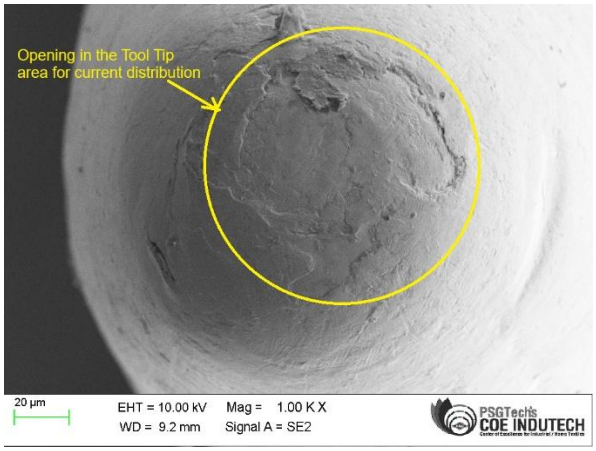


Figure 1. Palladium coated tool electrode

The preliminary experiments were conducted by varying one parameter at a time [Borgonovo, (2010)]. Totally 18 experiments (Table 1), $NaNO_3$ electrolyte with varying concentration was used for the experiments. The same process is repeated for the $NaNO_3$ electrolyte with complexing agent (sodium citrate). The $NaNO_3$ solution is added with 1% sodium citrate (Na_3Cit) in 1 liter of distilled water.

Table 1. Experimental parameters and output performances

Expt. Run	Voltage In Volts	Duty cycle (%)	Electrolyte Conc. (mol/L)	Electrolyte Conc. with (1%) Na_3Cit (mol/L)	MR µm/sec	MR of composite electrolyte µm/sec	OC µm	OC of composite electrolyte
1	6	90	0.41	0.001	0.198	0.225	343	302
2	7	90	0.41	0.001	0.238	0.278	323	293
3	8	90	0.41	0.001	0.269	0.309	284	265
4	9	90	0.41	0.001	0.298	0.362	260	241
5	10	90	0.41	0.001	0.347	0.439	235	220
6	11	90	0.41	0.001	0.417	0.521	221	204
7	11	40	0.41	0.001	0.167	0.185	360	330
8	11	50	0.41	0.001	0.194	0.219	336	310
9	11	60	0.41	0.001	0.219	0.253	294	262
10	11	70	0.41	0.001	0.245	0.278	274	242
11	11	80	0.41	0.001	0.278	0.321	250	230
12	11	90	0.41	0.001	0.298	0.347	238	218
13	11	90	0.12	0.001	0.198	0.231	350	326

14	11	90	0.18	0.001	0.214	0.269	336	310
15	11	90	0.24	0.001	0.238	0.298	322	290
16	11	90	0.29	0.001	0.269	0.379	296	266
17	11	90	0.35	0.001	0.347	0.439	252	231
18	11	90	0.41	0.001	0.439	0.463	230	211

THEORY OF MATERIAL REMOVAL REACTIONS

In this study two types of electrolytes were used namely $NaNO_3$, and sodium citrate ($Na_3C_6H_5O_7$) were used. The $NaNO_3$ electrolyte pprovides high ionic conductivity and supports stable anodic dissolution without aggressive pitting. The Chelates Fe^{3+}, Cr^{3+} and Ni^{2+} ions in sodium citrate (Na_3Cit), minimizes hydroxide precipitation, improves electrolyte stability, and enhances surface finish. The electrolyte dissociation equations are follows [da Silva et al.2019, Cheung and Williams (2015)]:

$$NaNO_3 \rightarrow Na^+ + NaNO_3^-$$

$$Na_3C_6H_5O_7 \rightarrow 3Na^+ + C_6H_5O_7^{3-}$$

Anode Reactions:

$$Fe \rightarrow Fe^{2+} + 2e$$

$$Fe \rightarrow Fe^{3+} + 3e$$

$$Cr \rightarrow Cr^{3+} + 3e$$

$$Ni \rightarrow Ni^{2+} + 2e^-$$

Overall anodic dissolution is

$$Fe - Cr - Ni \rightarrow Fe^{2+/3+} + Cr^{3+} + Ni^{2+} + e^-$$

Cathodic Reaction

$$2H_2O + 2e^- \rightarrow H_2 \uparrow + 2OH^-$$

Citrate complexation:

The dissolved metal ions immediately form soluble citrate complexes.

Iron: $Fe^{3+} + C_6H_5O_7^{3-} \rightarrow [Fe(C_6H_5O_7)]$

Chromium: $Cr^{3+} + C_6H_5O_7^{3-} \rightarrow [Cr(C_6H_5O_7)]$

Nickel: $Ni^{3+} + C_6H_5O_7^{3-} \rightarrow [Ni(C_6H_5O_7)]$

Hydroxide formation:

$$Fe^{3+} + 3OH^- \rightarrow Fe(OH)_3 \downarrow$$

$$Cr^{3+} + 3OH^- \rightarrow Cr(OH)_3 \downarrow$$

$$Ni^{2+} + 2OH^- \rightarrow Ni(OH)_2 \downarrow$$

Overall ECM reactions

$304SS + H_2O + NaNO_3 + Na_3C_6H_5O_7 \rightarrow Fe^{2+/3+} + Cr^{3+} + Ni^{2+} +$ metal citrate complexes $+ H_2 \uparrow$

INFLUENCE OF VOLTAGE ON MR AND OC

The machining rate increases steadily with increasing voltage from 6 V to 11 V for both electrolyte systems as shown in figure 2. This behavior is attributed to the increase in current density at higher voltages, which accelerates the anodic dissolution of the workpiece material according to Faraday's law of electrolysis. For the $NaNO_3$ electrolyte, the machining rate rises from 0.20 µm/s at 6 V to 0.42 µm/s at 11 V, indicating enhanced material removal due to increased electrochemical reaction kinetics**.** The highest machining rate of 0.52 µm/s is achieved at 11 V using the $NaNO_3$ + Na_3Cit electrolyte, representing about 24% higher machining rate compared to $NaNO_3$ alone at the same voltage. This demonstrates that the combination of a palladium-coated electrode and citrate-assisted electrolyte significantly enhances ECM performance by improving dissolution kinetics, electrolyte stability, and material removal efficiency.

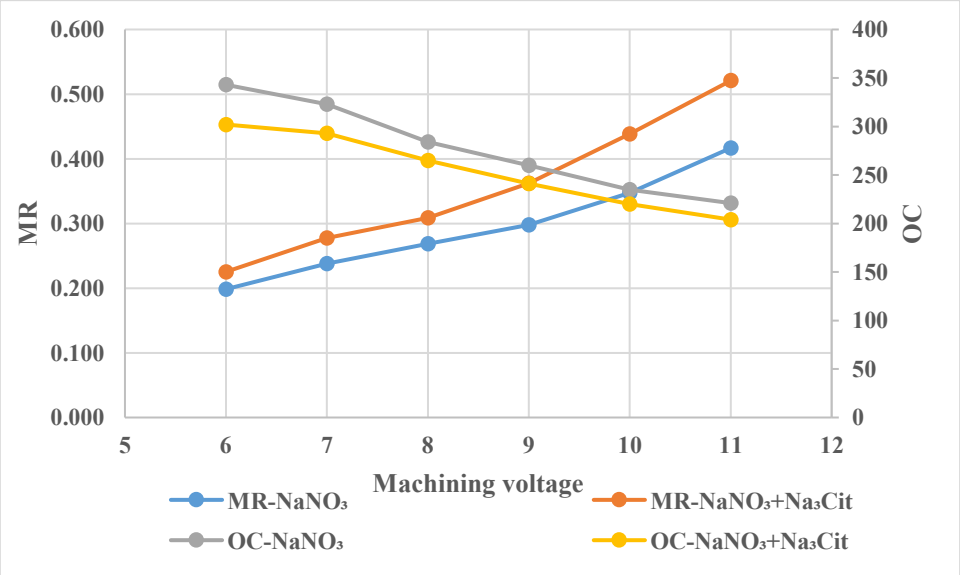


Figure 2 Graph for Voltage vs MR&OC

The figure 1 shows the OC fluctuation with machining voltage for $NaNO_3$ electrolyte and $NaNO_3$ + Na_3Cit electrolyte. As the applied voltage rises from 6 V to 11 V for both electrolytes, the OC steadily reduces, suggesting that dimensional accuracy improves at higher voltages. The OC for the $NaNO_3$ electrolyte drops by 35.6%, from roughly 343 µm at 6 V to 221 µm at 11 V. At the same time, the OC for the $NaNO_3$ + Na_3Cit electrolyte drops from 302 µm to 204 µm, or nearly 32.5%. Throughout the examined voltage range, the inclusion of trisodium citrate consistently results in lower OC values than the traditional $NaNO_3$ electrolyte. Because anodic dissolution is more widely distributed around the cutting zone at lower voltages (6–7 V), the

machining process shows relatively higher OC. Because of the slower electrolyte replenishment and less limited current distribution caused by the weaker electric field, material is removed beyond the specified machining boundary. Dimensional precision is consequently decreased when electrochemical dissolution is poorly localized. The ECM reaction gets more localized and stable as the voltage rises from 8 V to 11 V. Lateral dissolution is inhibited because the increased electric field speeds up the elimination of reaction products and improves electrolyte circulation within the IEG. As a result, the OC gradually decreases and the machined profile becomes thinner. Under the chosen experimental settings, the trend shows that increased voltage enhances machining precision. Trisodium citrate's function as a complexing and buffering agent is responsible for the $NaNO_3$ + Na_3Cit electrolyte excellent performance. To stop dissolved metallic ions from precipitating inside the machining gap, trisodium citrate combines with them to produce soluble metal-citrate complexes. This reduces the buildup of sludge, enhances electrolyte conductivity, and promotes even current distribution. Furthermore, citrate's buffering function lowers localized corrosion and inhibits stray anodic dissolution, all of which contribute to a stable electrolyte pH. Compared to the $NaNO_3$ electrolyte alone, material removal becomes more localized as a result, resulting in much less OC.

INFLUENCE OF DUTY CYCLE ON MR AND OC

Figure 3 shows that the highest machining rate of 0.35 μm/s is achieved at 90% duty cycle using the $NaNO_3$ + Na_3Cit electrolyte, whereas the $NaNO_3$ electrolyte attains only about 0.30 μm/s under the same conditions. The addition of sodium citrate provides an improvement of nearly 17–20% in machining rate across the investigated duty cycle range. At higher duty cycles (80–90%), the difference between the two electrolytes became more noticeable, suggesting that Na_3Cit has a more positive impact when current density is higher. The electrolyte undergoes increased ionic activity and heat generation at larger pulse-on times, but the inclusion of Na_3Cit stabilizes the electrolyte and maintains effective dissolution, resulting in a machining rate that is about 15–20% higher than that achieved with $NaNO_3$ alone [Guodong et al.2016]. A duty cycle range of 40–90% was chosen for further trials based on these first studies since it offered stable machining conditions and a steady increase in machining rate without showing signs of process instability. Furthermore, the $NaNO_3$ + Na_3Cit electrolyte showed better machining performance and was selected for additional optimization research.

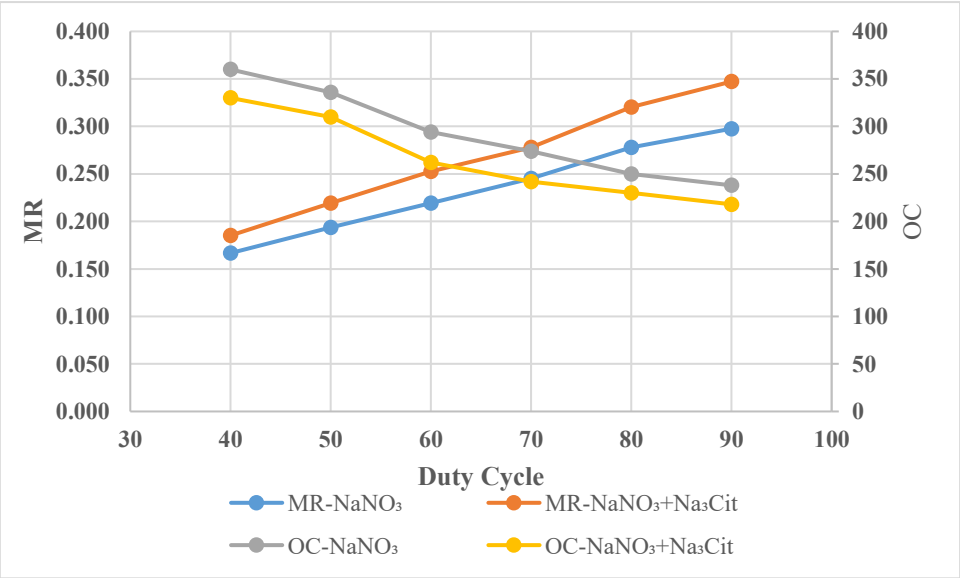


Figure 3. Graph for Duty cycle vs MR&OC

The figure 3 shows the fluctuation of OC with duty cycle for machining with $NaNO_3$ and $NaNO_3$ + Na_3Cit electrolytes. For both electrolyte situations, the OC continuously drops as the duty cycle increases. The OC is roughly 360 µm for $NaNO_3$ and 330 µm for the $NaNO_3$ + Na_3Cit electrolyte at a duty cycle of 40%. The OC drops to roughly 240 µm and 220 µm, respectively, when the duty cycle rises to 90%. This reduces the amount of sidewall material removal and enhances dimensional accuracy by minimizing undesired lateral current dispersion. The OC is significantly reduced over the whole duty cycle range when Na_3Cit is added. By controlling the dissolution of metal ions and preserving a more consistent electrolyte chemistry, Na_3Cit functions as a complexing and buffering agent. It makes it easier to remove reaction products from the machining zone and inhibits stray electrochemical reactions. As a result, compared to pure $NaNO_3$, the electrolyte incorporating Na_3Cit generates a more restricted current distribution, which results in less lateral dissolution and OC. At greater duty cycles, the two electrolytes' differences become more apparent. The $NaNO_3$ + Na_3Cit electrolyte produces almost 20 µm less OC than the $NaNO_3$ electrolyte at 90% duty cycle, suggesting that the combination of optimal pulse settings and electrolyte alteration greatly improves machining precision.

INFLUENCE OF ELECTROLYTE CONCENTRATION ON MR AND OC

The highest machining rate of 0.46 µm/s is obtained at 0.41 mol/L using the $NaNO_3$ + Na_3Cit electrolyte, while the $NaNO_3$ electrolyte achieves about 0.44 µm/s under the same conditions as depicted in figure 4. The citrate-assisted electrolyte provides superior machining performance throughout the concentration range, particularly in the medium concentration region (0.24–0.35 mol/L), where enhanced complexation and dissolution kinetics contribute significantly to material removal. The palladium-coated electrode contributes significantly to improving machining performance in addition to the electrolyte impact. Excellent electrical conductivity and catalytic activity toward the hydrogen evolution reaction taking place at the cathode are features of palladium. By encouraging quick hydrogen evolution with less polarization, the coating lessens gas buildup on the electrode surface and guarantees a more consistent current distribution across the machining zone. The workpiece dissolves

electrochemically steadily because of this uniform current distribution, which also reduces localized current concentration.

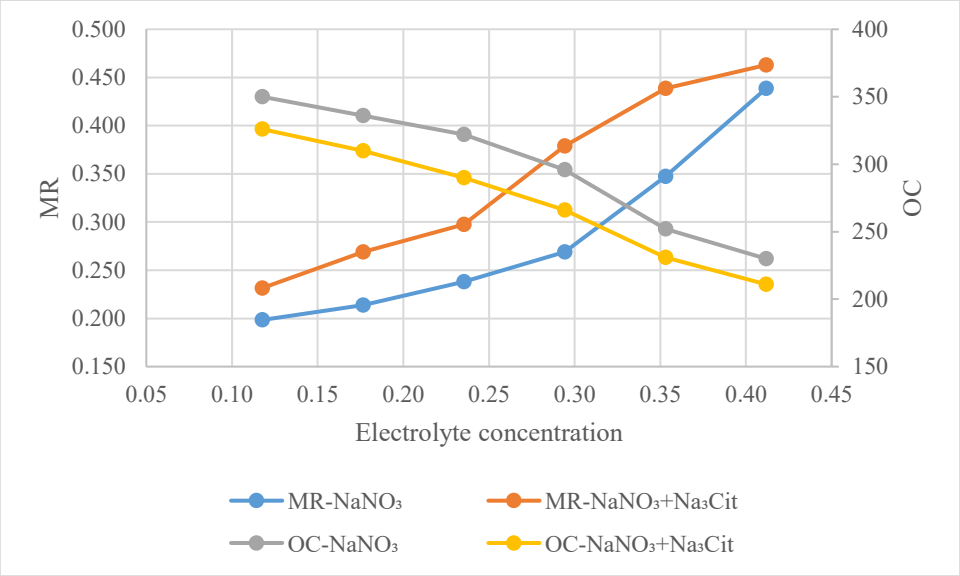


Figure 4 Graph for Electrolyte Concentration vs MR & OC

The graphic (figure 4) shows how OC varies with electrolyte content for $NaNO_3$ and $NaNO_3$ + Na_3Cit electrolytes. OC for both electrolytes continuously decreases when the electrolyte concentration is raised from 0.12 to 0.41 mol/L. Over the whole concentration range, however, adding Na_3Cit consistently results in a lower OC than the traditional $NaNO_3$ electrolyte. The OC is roughly 350 µm for $NaNO_3$ and 325 µm for the $NaNO_3$ + Na_3Cit electrolyte at the lowest electrolyte concentration of 0.12 mol/L. The OC drops to approximately 230 µm and 210 µm, respectively, as the concentration rises to 0.41 mol/L. This corresponds to an overall reduction of approximately 34% for $NaNO_3$ and 35% for the mixed electrolyte, demonstrating the effectiveness of increasing electrolyte conductivity and introducing Na_3Cit [Upadhyay et al. (2025)]

The reduction in OC with increasing electrolyte concentration is primarily attributed to the enhanced ionic conductivity of the electrolyte, which promotes more stable current flow and localized anodic dissolution [Kumaar et al.2022, Maniraj and Thanigaivelan, (2019)]. At higher concentrations, the electrolyte efficiently removes machining by-products, hydrogen bubbles, and heat from the IEG, resulting in a more uniform electric field and minimizing undesirable lateral dissolution of the workpiece. Consequently, the machined cavity closely follows the geometry of the tool, leading to improved dimensional accuracy. The $NaNO_3$ + Na_3Cit electrolyte demonstrates consistently decreased OC because Na_3Cit functions as a complexing and buffering agent. By forming soluble complexes with dissolved metal ions, citrate ions keep the machining gap cleaner and stop the metal ions from redepositing on the workpiece surface. Furthermore, Na_3Cit stabilizes the anodic dissolving process, reduces stray current effects, and moderates localized current density. Together, these factors enhance machining accuracy and decrease side-wall material removal.

ANALYSIS OF MACHINE HOLE FOR $NANO_3$ ELECTROLYTE

The SEM picture shown in figure 5 depicts the rough surface with irregular granular forms and isolated deposits on the periphery of the machined hole. These characteristics are mainly explained by the buildup of corrosion products, passive oxide coatings, and machining muck produced during electrochemical dissolution. Iron, chromium, and nickel atoms from the AISI 304 SS oxidize into Fe^{3+}, Cr^{3+}, and Ni^{2+} ions during machining [Deepak & Hariharan (2022)]. These dissolved metal ions often react with hydroxyl ions produced at the cathode in the absence of an efficient complexing agent, creating insoluble hydroxides that may stick to the machined surface and degrade the surface finish.

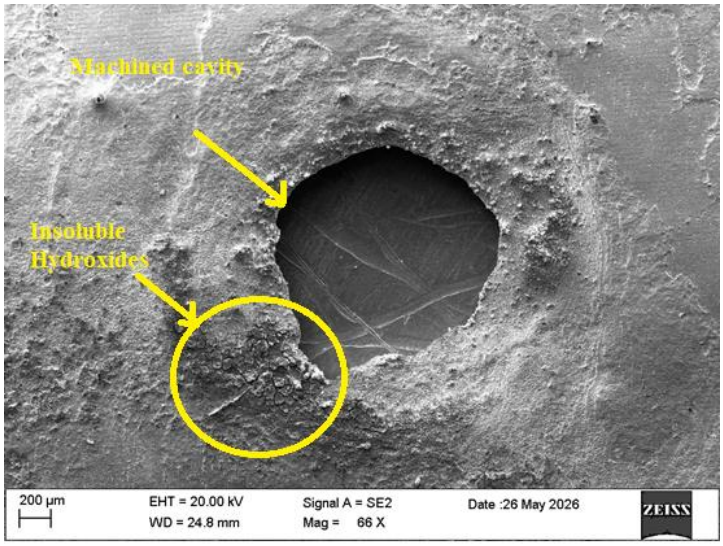


Figure 5. SEM of hole with insoluble hydroxides

Figure 6 shows the presence of granular and flaky deposits around the hole periphery, especially on the lower-left side of the machined region. These deposits are explained by the buildup of corrosion products and electrochemical sludge created during anodic dissolution. The main alloying components of AISI 304 SS oxidize during machining. Insoluble metal hydroxides are created when the dissolved metal ions combine with hydroxyl ions produced at the cathode. The rough and flaky appearance shown in the SEM image is caused by these hydroxide precipitates building up surrounding the machined area as machining muck. Localized fluctuations in current density and decreased machining uniformity may arise from the deposited products partially obstructing electrolyte circulation within the IEG.

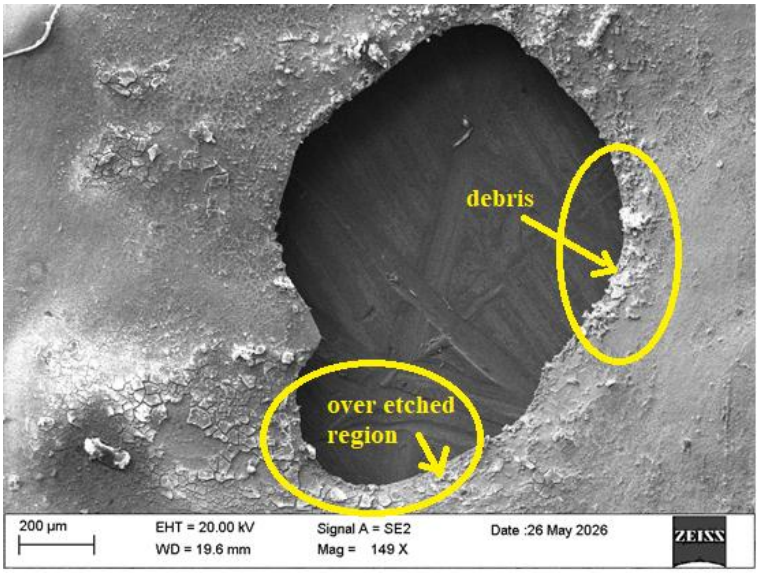


Figure 6. SEM of hole with over etched surface

ANALYSIS OF MACHINE HOLE FOR $NANO_3$ + NA_3CIT ELECTROLYTE

A well-defined, nearly circular hole with relatively consistent geometry is shown in the SEM image (figure 7), suggesting stable anodic dissolution during the machining process. The hole's interior surface is smooth and devoid of flaws like microcracks, and deposited regions indicating that material removal was solely accomplished by electrochemical dissolution. The fine polishing lines that are visible inside the machined cavity show little surface deterioration and match the workpiece's initial surface finish. The area around the machined hole shows noticeably fewer sludge deposits and corrosion products when compared to machining with $NaNO_3$ alone. The hole boundary shows very little fine granular residue, indicating effective removal of dissolved metal ions from the IEG.

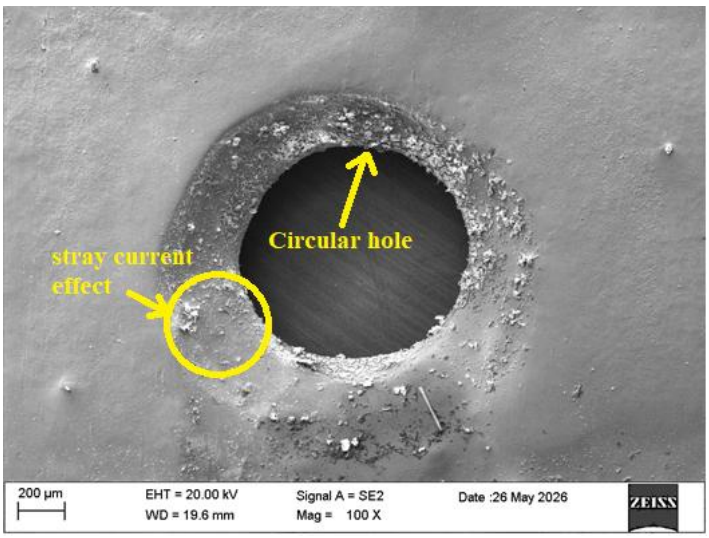


Figure 7. SEM of hole machined with composite electrolyte

A clearly defined, almost round hole with a relatively smooth and uniform boundary is visible in the SEM image (figure 8), suggesting regulated anodic dissolution throughout the machining process. The machined hole interior surface is smooth and devoid of micro spark affected areas, and debris attached region, indicating that material removal was solely accomplished by electrochemical dissolution. The polishing marks that are visible inside the cavity match the workpiece initial surface quality, demonstrating that the ECM process maintained the substrate's metallurgical integrity. The current micrograph shows significantly less deposition of sludge and corrosion products at the hole periphery than the specimen machined using $NaNO_3$ alone [Maniraj and Thanigaivelan, 2019].

Stray anodic dissolution was considerably decreased, as evidenced by the homogeneous circular geometry and limited OC region surrounding the machined hole. Better edge definition and increased dimensional accuracy were the outcomes of the electrochemical reaction's improved localization [Maniraj et al.2023]. Additionally, the lack of large, agglomerated corrosion products shows that Na_3Cit efficiently reduces passive layer buildup and promotes the workpiece material's continuous breakdown. When compared to sodium nitrate alone, the combined electrolyte system offers better machining performance, as confirmed by the overall surface morphology. Cleaner machining conditions, better electrolyte flow, less sludge formation, and increased surface integrity result from the synergistic effect of Na_3Cit, which complexes dissolved metal ions and stabilizes the electrolyte, and $NaNO_3$, which offers strong ionic conductivity.

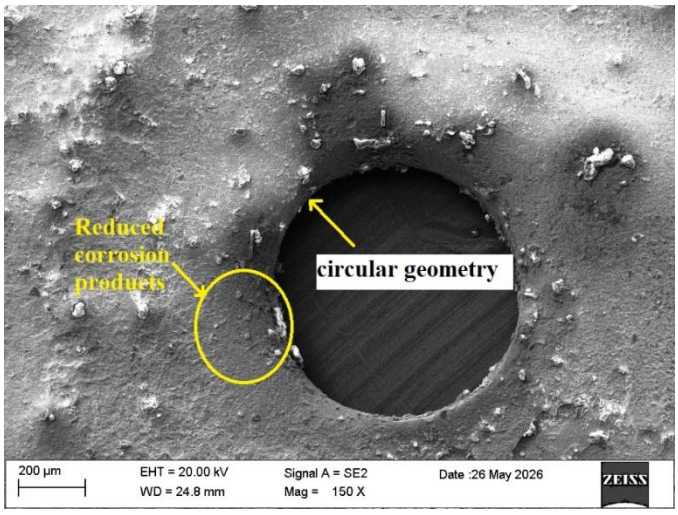


Figure 8. SEM picture of hole with circular geometry

Conclusions

The experimental study shows that adding sodium citrate to NaNO3 substantially enhances the ECM performance of AISI 304 stainless steel when using a palladium-coated tool electrode. Based on the quantitative results, the following conclusions can be drawn:

1. The machining voltage significantly affected material removal. Raising the voltage from 6 to 11 V increased the MR of $NaNO_3$ from 0.20 to 0.42 µm/ s. At the same conditions, the $NaNO_3$ + Na_3Cit electrolyte reached a peak MR of 0.52 µm/s at 11 V, about 24% greater than the value observed with $NaNO_3$ alone.

2. Accuracy in dimensions improved significantly as voltage increased. For $NaNO_3$, the OC dropped from about 343 µm at 6 V to 221 µm at 11 V, representing a 35.6% decrease. Using $NaNO_3$ and Na_3Cit, the OC dropped from about 302 to 204 µm, a 32.5% decrease.
3. A higher duty cycle improved MR but decreased OC. At a 90% duty cycle, the $NaNO_3$ + Na_3Cit mixture achieved an MR of about 0.35 µm/s, compared to 0.30 µm/s for $NaNO_3$ alone. Across the tested duty-cycle range, sodium citrate resulted in roughly a 17-20% increase in MR. At the same 90% duty cycle, OC dropped to about 220 µm when using $NaNO_3$ + Na_3Cit, compared to 240 µm with $NaNO_3$ alone, resulting in an absolute decrease of roughly 20 µm. This verifies enhanced localization of electrochemical dissolution within the citrate-assisted electrolyte.
4. The concentration of electrolyte also improved machining performance. At the highest tested concentration of 0.41 mol/L, the $NaNO_3$ + Na_3Cit electrolyte attained an MR of 0.46 µm/s, compared to roughly 0.44 µm/s for $NaNO_3$ alone Raising the electrolyte concentration from 0.12 to 0.41 mol/ L decreased OC from about 350 to 230 µm in $NaNO_3$, representing a 34% drop, while in $NaNO_3$ + Na_3Cit, OC fell from around 325 to 210 µm, indicating a 35% reduction.
5. The SEM analysis supported the machining measurements. Holes made using $NaNO_3$ by itself showed granular deposits, insoluble hydroxides, machining sludge, uneven edges, and areas of excessive etching; in contrast, the $NaNO_3$ + Na_3Cit electrolyte produced cleaner, nearly circular holes with smoother edges, less corrosion-product buildup, sharper edge definition, and less unwanted dissolution.
6. Overall, the experimental results establish $NaNO_3$ + Na_3Cit as the superior electrolyte system within the investigated parameter ranges. The highest reported machining rate was 0.52 µm/ s at 11 V, while low OC values of approximately 204 µm at 11 V, 220 µm at 90% duty cycle, and 210 µm at 0.41 mol/ L electrolyte concentration were obtained with the citrate-assisted electrolyte.

Declaration

Ethics Approval and consent to participate

Not applicable

Consent for Publication

All authors consent to the publication of this manuscript

Competing interests

The authors declare that they have no competing interests

Authors' contributions

NSCB, SKG (First author and Second author) has drafted the manuscript, conception, design of the work; TR and SD (Third and fourth authors) did the analysis, conception, interpretation of data; SK, SL (fifth and sixth authors) has reviewed the article, analyzed, and TR (seventh author) concluded the obtained results and corresponds. All authors read and approved the final manuscript.

Availability of supporting data

The data will be made available on request

Funding

There is no funding received for this research.

Acknowledgement

Not applicable

REFERENCES

1. Sethi, A., Acharya, B. R., & Saha, P. (2022). Study of the electrochemical dissolution behavior of Nitinol shape memory alloy in different electrolytes for micro-ECM process. The International Journal of Advanced Manufacturing Technology, 121(9), 7019-7035.
2. Gokulanathan, L., & Annamalai, J. (2024). Experimental Investigation of Micro-ECM On Monel 400 Alloy Using Particles Mixed Electrolyte, Chemical Industry & Chemical Engineering Quarterly, 30(1), 81-88.
3. Zishanur Rahman, M., Das, A. K., & Chattopadhyaya, S. (2022). A comparative study of NaOH and KOH electrolytes in micro-ECM. Advances in Materials and Processing Technologies, 8(4), 4181-4193.
4. Sriram, D., Sunil, B. D. Y., Jeyakrishnan, S., Rakesh, C., Vijayakumar, S., Kumar, A. Sehgal, L. (2025). Investigation of different electrolyte effects on micro-hole machining of scrapped wheel alloy. Results in Surfaces and Interfaces, 18, 100429.
5. He, J., Wang, Z., Zhou, W., Jian, Y., & Zhou, L. (2023). Electrolytic characteristics of microhole array manufacturing using polyacrylamide electrolyte in 304 stainless steel. Micromachines, 14(10), 1808.
6. Kumaar, J. R. K. V., Thanigaivelan, R., & Soundarrajan, M. (2022). Effect of different electrolytes on electrochemical micro-machining of SS 316L. Chemical Industry & Chemical Engineering Quarterly, 28(4), 329-337.
7. Najm, V. N., Abdulrazaq, M. M., & Ahmed, A. M. S. (2025). Enhancing surface integrity of 316 SS with ecofriendly electrolyte in electrochemical machining. *Advances in Science and Technology. Research Journal*, *19*(12).
8. Gunasekaran, P. K., Rajasekaran, T., & Rangasamy, V. (2026). Electrochemical machining with ethylene glycol mixed electrolyte on inconel 718. Chemical Industry & Chemical Engineering Quarterly, 32(4), 321-330.
9. Gunasekaran, S., Periyagounder, S., & Subramaniam, M. (2023). Enhancing micromachining precision with novel electrolyte combinations: an investigation. Journal of Ceramic Processing Research, 24(4), 705-713.
10. Sankar, M., Gnanavelbabu, A., Rajkumar, K., & Thushal, N. A. (2017). Electrolytic concentration effect on the abrasive assisted-electrochemical machining of an aluminum–boron carbide composite. Materials and Manufacturing Processes, 32(6), 687-692.

11. Janardhanan, D., & Perianna, H. (2024). Experimental investigation on the suitability of dual fluid system-assisted ECM (DF-ECM) and the influence of magnet in machining of SS304. The International Journal of Advanced Manufacturing Technology, 130(7), 3819-3836.
12. Ayyappan, S., & Sivakumar, K. (2014). Experimental investigation on the performance improvement of electrochemical machining process using oxygen-enriched electrolyte. The International Journal of Advanced Manufacturing Technology, 75(1), 479-487.
13. Dong, Q., Jiang, W., Wang, Y., Zhang, L., Tan, J., Xiong, X., ... & Zhang, W. (2026). Ultra-high aspect ratio micro holes drilling by laser and electrochemical machining via enhanced mass transport in the machining gap. *The International Journal of Advanced Manufacturing Technology*, *143*(3), 1657-1677.
14. Qin, G., Li, S., Li, M., Peng, H., Niu, S., Li, X., ... & Ming, P. (2024). Electrochemical machining of micro-pit arrays on a GH4169 alloy with a roll-print mask using a C6H5Na3O7-containing nano3 mixed electrolyte. *Micromachines*, *15*(10), 1253.
15. Borgonovo, E. (2010). A methodology for determining interactions in probabilistic safety assessment models by varying one parameter at a time. Risk Analysis: An International Journal, 30(3), 385-399.
16. da Silva, G. P., de Lima, R. N., Santos, F. J. N., de Menezes, F. P. S., Morais, L. P. L., & da Silva Filho, L. F. (2019). Influence of the complexing agent sodium citrate on the chemical composition, surface morphology and corrosion resistance of Ni–Fe electrodeposits. *Transactions of the IMF*, *97*(5), 230-236.
17. Cheung, P. C., & Williams, D. R. (2015). Separation of transition metals and chelated complexes in wastewaters. *Environmental Progress & Sustainable Energy*, *34*(3), 761-783.
18. Guodong, L., Yong, L., Quancun, K., & Hao, T. (2016). Selection and optimization of electrolyte for micro electrochemical machining on stainless steel 304. Procedia Cirp, 42, 412-417.
19. Upadhyay, R. K., Majhi, S. S., Mahapatra, S. S., Yadav, N., Chakraborty, A. K., Singh, A. C., & Kumar, B. (2025). A comparative study on material removal rate and surface roughness during electrochemical machining of 100Cr6 steel in oxidizing and reducing electrolytic environments. Proceedings of the Institution of Mechanical Engineers, Part E: Journal of Process Mechanical Engineering, 09544089251316751.
20. Kumaar, J. R. K. V., Thanigaivelan, R., & Soundarrajan, M. (2022). Effect of different electrolytes on electrochemical micro-machining of SS 316L. Chemical Industry & Chemical Engineering Quarterly, 28(4), 329-337.
21. Maniraj, S., & Thanigaivelan, R. (2019). Effect of electrode heating on performance of electrochemical micromachining. *Materials and Manufacturing Processes*, *34*(13), 1494-1501.
22. Maniraj, S., & Thanigaivelan, R. (2019). Optimization of electrochemical micromachining process parameters for machining of AMCs with different% compositions of GGBS using Taguchi and TOPSIS methods. *Transactions of the Indian Institute of Metals*, *72*(12), 3057-3066.
23. Maniraj, S., Thanigaivelan, R., Gunasekaran, K., & Saravanan, K. G. (2023). Optimization of process parameters in electrochemical micromachining of amcs by using different techniques of weight evaluation. *Advances in Materials Science and Engineering*, *2023*(1), 1366857.

24. Deepak, J., & Hariharan, P. (2022). Study on the influence of auxiliary electrode and magnet on electrochemical machining of SS304 using NaCl and NaNO3. Surface Topography: Metrology and Properties, 10(1), 015045.